SAND76-8204
Unlimited Release

Theoretical Calculation of Raman Scattering Cross Sections for Use in Flame Analysis

C. F. Coll, C. F. Melius

Prepared by Sandia Laboratories, Albuquerque, New Mexico 87115 and Livermore, California 94550 for the United States Energy Research and Development Administration under Contract AT (29-1)-789

Printed February 1976

Sandia Laboratories

SF 2900 Q(7-73)

When printing a copy of any digitized SAND Report, you are required to update the markings to current standards.

Issued by Sandia Laboratories, operated for the United States Energy Research and Development Administration by Sandia Corporation.

NOTICE

This report was prepared as an account of work sponsored by the United States Government. Neither the United States nor the United States Energy Research and Development Administration, nor any of their employees, nor any of their contractors, subcontractors, or their employees, makes any warranty, express or implied, or assumes any legal liability or responsibility for the accuracy, completeness or usefulness of any information, apparatus, product or process disclosed, or represents that its use would not infringe privately owned rights.

SAND76-8204
Unlimited Release
Printed February 1976

THEORETICAL CALCULATION OF RAMAN SCATTERING CROSS SECTIONS FOR USE IN FLAME ANALYSIS†

C. F. Coll and C. F. Melius
Sandia Laboratories, Livermore, CA 94550

ABSTRACT

The laser Raman scattering analysis of combustion flames requires a knowledge of the scattering cross sections for a variety of molecular species. Since cross sections are known for only the most common and most stable of molecules (e.g., N_2, O_2 and H_2), we have initiated a program to calculate cross sections for other molecules of interest to combustion analysis. In this paper we present theoretically-determined cross sections for H_2, N_2, OH, LiH, and O_2. Comparison with the few experimentally determined cross sections indicate that our theoretical approach is a reliable method for determining Raman scattering cross sections for those molecules whose cross-sections cannot be readily determined experimentally.

†This work is supported by the U. S. Energy Research and Development Administration.

I. INTRODUCTION

The Raman scattering of laser light has been a useful technique in the determination of molecular structure.[1] Recently, it has been applied as a probe in combustion research to analyze macroscopic properties of combustion flames.[2] In particular, Sandia Laboratories[3] has initiated a research effort to determine the time-dependent temperature and concentration profiles of the various molecular species present in combustion flames.

Sandia's Raman scattering experiments focus an Ar ion laser (4880 Å) at a specific spot in the combustion flame and measure the intensity of the scattered light from a particular molecular species. Knowing the intensity of the incident light I_{inc} and the scattered light I_{scatt} allows one to determine the concentration of a given molecular species N; i.e.,

$$N = \frac{I_{scatt}}{I_{inc}\,\sigma_{Raman}}$$

where σ_{Raman} is the Raman scattering cross section for a particular molecular species.

---

1. See, for example, G. Herzberg, Infrared and Raman Spectra of Polyatomic Molecules, D. Van Nostrand, Inc., New York, 1956.

2. See, for example, Laser Raman Gas Diagonstics (M. Lapp, C. M. Penney, eds.), Plenum Press, New York (1974).

3. For a review of Sandia's work in this area, see R. E. Setchell, "Analysis of Flame Emissions by Laser Raman Spectroscopy," SLL-74-5244.

The Raman scattering technique, therefore, requires a knowledge of the Raman scattering cross section σ_{Raman} for the various molecular species occurring in combustion flames. However, Raman scattering cross sections are known for only a few stable molecules, such as H_2, N_2, O_2, NO, CO, and H_2O. In combustion flames, on the other hand, many of the molecular species of critical importance to the understanding of the combustion process, are of an unstable, transient nature. For these short-lived species, the experimental determination of the Raman cross sections is non-existent, principally because these highly reactive molecules are difficult to isolate for purposes of measurement. Thus, for these reactive species, theoretical calculations are needed to provide Raman scattering cross sections which would be difficult or impossible to obtain experimentally.

To develop an ability to determine the Raman cross sections for such molecular species, we have undertaken a theoretical investigation of scattering cross-sections for a number of diatomic molecules. In the course of our investigation, we have applied the rather sophisticated techniques of quantum chemistry. The simplest ab initio treatment (the Hartree-Fock method) considers each electron in the system to move independently in the average Coulomb field of the other electrons. This independent electron approach ignores the tendency of the electrons to correlate their motion in such a way as to reduce their Coulomb repulsion. We have found that in order to provide a reliable treatment for diatomic molecules we have had to abandon the one electron picture of the Hartree-Fock treatment by including those correlation effects appropriate for describing molecular dissociation. The comparison between experimental data, where it exists, and our calculated results has provided an assessment of the validity of our treatment which we have then applied with confidence to those molecules for which little, if any, cross section data exists.

II. RAMAN SCATTERING PROCESS

The Raman scattering process consists basically of irradiating a system of molecules with monochromatic radiation and measuring the intensity, polarization, and frequency of the radiation scattered by the sample. The scattering process can be considered as a means of probing, on a microscopic scale, the properties of the sample. We indicate schematically in Figure 1 the experimental geometry frequently used in light scattering experiments. The laser light is incident along the (-x) direction and the scattered light is observed at 90° to the incident beam. If we assume that the incident radiation is polarized in the z-direction, the scattered radiation can be polarized in either the x or z direction. This is illustrated in Figure 2. In Sandia's experiments one measures the sum of the light intensity scattered parallel and perpendicular to the polarization of the incident beam. The ratio of the intensity of scattered light to that of the incident light is then a quantitative measure of the scattering strength of the sample. If we know the scattering strength of each molecule, we can then determine the number of molecules of a given species present in the sample.

To gain some insight into the molecular characteristics which are probed by light scattering, we begin with a description of the scattering process from a classical point of view. This will enable us to introduce the pertinent physical concepts and the terminology used in laser Raman scattering. The classical description will indicate what molecular quantities must be determined in order to describe quantitatively the scattering strength of a given molecule. The actual calculation of these quantities requires a quantum-mechanical description which we present in Section IV.

III. CLASSICAL TREATMENT OF RAMAN SCATTERING

From a classical point of view the Raman scattering process can be thought of as one in which the incident radiation induces a dipole moment $\vec{M}$ in a molecule. The induced dipole moment then radiates as a classical oscillator. What is of physical interest, then, is the intensity, frequency, and polarization of this radiated energy.

The dipole moment induced in the molecule is related to the electric field vector of the incident radiation $\vec{E}_{inc}$ by an expression of the form

$$\vec{M} = \overleftrightarrow{\alpha} : \vec{E}_{inc} \tag{1}$$

The second-rank tensor $\overleftrightarrow{\alpha}$ is called the polarizability of the molecule. For illustrative purposes, we will consider the scattering system to be a simple diatomic molecule such as H_2 or N_2. For such molecules the polarizability tensor is symmetric and the two principal values of the tensor are denoted $\alpha_{||}$ and $\alpha_{\perp}$. Physically these quantities represent the dipole moment induced in the molecule when an electric field of unit magnitude is applied parallel or perpendicular, respectively, to the axis of the molecule.

In writing Eq. (1) we have assumed that the magnitude of the incident electric field is small enough so that the induced dipole moment varies <u>linearly</u> with the incident field. For application to laser Raman scattering we may assume that the incident electric field E_{inc} is monochromatic with a frequency ν_{inc}. Thus, $\vec{E}_{inc}$ is given by

$$\vec{E}_{inc} = \vec{E}^{(o)}_{inc} \cos (2\pi\nu_{inc} t). \tag{2}$$

From Eq. (1) and Eq. (2) we see that if the polarizability were independent of time the induced dipole moment would oscillate at the frequency ν_{inc}. We

will see below that $\overleftrightarrow{\alpha}$ changes with time (due to the motion of the nuclei comprising the molecule) so that in general

$$\vec{M} = \vec{M}_o \cos\ (2\pi\nu_{scatt}t), \tag{3}$$

where $\vec{M}_o$ is the amplitude and ν_{scatt} the frequency of the induced dipole moment. The average rate of total radiation from such an oscillator is given by[4]

$$I = \frac{16\pi^4\nu^4_{scatt}}{3c^2} M_o^2 \tag{4}$$

In order to relate ν_{scatt} and M_o to the properties of the scattering molecule we must consider how the polarizability changes with time. In general, the polarizability will vary with the geometry of the molecule, i.e., it will depend on the vibrational or other motion of the nuclei. If the displacements of the nuclei from their equilibrium positions are small, we may write each component of the polarizability tensor as a power series expansion about the equilibrium geometry

$$\alpha(R) = \alpha(R_e) + \frac{d\alpha}{dR}\Big|_{R_e} (R-R_e) + \ . \ . \ . \tag{5}$$

where R_e is the equilibrium value of the internuclear separation R. If we assume that the vibration of the nuclei is simple harmonic with frequency ν_{mol} we may write

$$R - R_e = R_o \cos 2\pi\nu_{mol}t \tag{6}$$

4. E. B. Wilson, Jr., Decius, J. C., and Cross, P. C., Molecular Vibrations, McGraw Hill, New York, 1955.

where R_o is the amplitude of vibration. Substituting this expression into Eq. (5) we find

$$\alpha(R) = \alpha_o + \alpha_1 \cos 2\pi\nu_{mol}t \tag{7a}$$

with

$$\alpha_o = \alpha(R_e) \tag{7b}$$

$$\alpha_1 = \frac{d\alpha}{dR}\Big|_{R_e} R_o \tag{7c}$$

The physical content of Eq. (7) is that the molecular polarizability is modulatec by the vibration of the molecule. If it is assumed that the field induces an oscillating dipole moment which is in phase with and parallel to the incident field then we find from Eq. (1)

$$M = \alpha_o E_{inc}^{(o)} \cos 2\pi\nu_{inc}t + \alpha_1 E_{inc}^{(o)} \cos 2\pi\nu_{inc}t \cos 2\pi\nu_{mol}t \tag{8a}$$

or

$$M = \alpha_o E_{inc}^{(o)} \cos 2\pi\nu_{inc}t + \frac{1}{2}\alpha_1 E_{inc}^{(o)} \cos 2\pi\,(\nu_{inc} + \nu_{mol})\,t + \frac{1}{2}\alpha_1 E_{inc}^{(o)} \cos 2\pi\,(\nu_{inc} - \nu_{mol})\,t\,. \tag{8b}$$

The induced dipole moment can, therefore, be regarded as the superposition of three periodically changing moments having frequencies ν_{inc}, $(\nu_{inc} + \nu_{mol})$, and $(\nu_{inc} - \nu_{mol})$, respectively. They radiate light of corresponding frequencies which constitute the Rayleigh line, the anti-Stokes Raman line and the Stokes-Raman, line respectively.

There are two main points to be made about Eq. (8). First, while it is the polarizability of the molecule which gives rise to Rayleigh scattering ($\nu_{scatt} = \nu_{inc}$), it is the *change* in the polarizability during molecular

motion which is responsible for the Raman effect ($\nu_{scatt} = \nu_{inc} \pm \nu_{mol}$). Second, the frequency shift measured in Raman scattering is related to an internal vibration frequency of that molecule which scatters the light. Since the internal frequency is specific to the molecule, its experimental measurement serves to identify the molecular species present in the flame.

So far we have assumed that the vibrational motion is harmonic. In reality, there is always some anharmonicity to the motion. A principal manifestation of this anharmonicity is that ν_{mol} depends on the thermal state of the vibrating molecule. Thus, the observation of the scattered light intensity at various frequencies enables one to measure quantitatively the temperature distribution of a given molecular species at various positions in the flame.

In summary, then, when light is scattered from a molecule the frequency of the scattered light may be shifted from that of the incident light. The shift is given by a frequency associated with an internal motion of the molecule. The intensity of this shifted radiation is determined by how strongly the polarizability of the molecule changes during the internal motion. For concentration and temperature analyses of flames, we must know both the shifts and associated polarizability changes. For some molecules these parameters can be determined experimentally. For other, short-lived molceular species, however, theoretical calculation provides the only avenue for determining these quantities.

While classical theory has indicated which parameters determine the scattered intensity; i.e., $\underline{\nu_{mol}}$ and α_1, it provides no scheme to calculate them. We, therefore, must apply a quantum mechanical treatment to determine these quantities.

IV. QUANTUM MECHANICAL TREATMENT OF RAMAN SCATTERING

Quantum mechanically the Raman scattering process is understood as the scattering of a photon accompanied by the change of internal state of the scattering molecule. The change in energy of the photon is compensated by an accompanying change in the energy state of the molecule. The initial and final states of the molecule are described by wavefunctions Ψ_i and Ψ_f, respectively. These wavefunctions depend on the electronic, vibrational, and rotational motion of the molecule. To first order, these can be treated separately, i.e. we can write

$$\Psi_j = \Psi_e (\vec{r}; R) \Psi_{VJ}(R) \Psi_J (\theta, \phi), \; j = i \text{ or } f. \tag{9}$$

The electronic wavefunction $\Psi_e (\vec{r},R)$ depends explicitly on the electronic coordinates, $\vec{r}$, and implicity on the internuclear separation R. The vibrational wavefunction Ψ_{VJ} (R) and the rotational wavefunction $\Psi_J (\theta,\phi)$ are then defined for a particular electronic energy state.

The intensity of the scattered light I_{scatt} is proportional to the intensity of incident light I_{inc}, the number of molecules, N, of a particular molecular species in the initial vibrational-rotational state, and the Raman scattering cross section σ_{Raman}

$$I_{scatt} = I_{inc} \, \sigma_{Raman} \, N \tag{10}$$

where for transitions between states Ψ_i and Ψ_f

$$\sigma_{Raman} = \frac{2^7 \pi^5}{3c^4} \nu^4_{scatt} \, | \alpha_{if} |^2 \tag{11}$$

Eq. (11) is similar to (4) except that M_0^2 is replaced by the transition probability $|\alpha_{if}|^2$ where α_{if} is the matrix element of the polarizability tensor between the initial and final states of the molecule.

Note that it is the matrix element α_{if} which plays the same role quantum mechanically as α_0 or α_1 [see Eq. (7)] does classically. Thus, if the initial and final molecular state are identical, α_{if} plays the role of α_0. For the case of Raman scattering ($\Psi_i \neq \Psi_f$) α_{if} can be identified with α_1, the change of polarizability.

For purposes of flame analysis, we need consider only transitions within the same electronic and rotational state (Q-branch Raman scattering). For these transitions, the matrix element α_{if} becomes

$$\alpha_{if} = \int dR \sin\theta d\theta d\phi \Psi_{V+1,J}(R)\Psi_J(\theta,\phi)\alpha(R)\Psi_{V,J}(R)\Psi_J(\theta,\phi) \qquad (12)$$

It should be noted that $\alpha(R)$ is really a tensor quantity and Eq. (12) holds for each tensor component.

Thus, if one can calculate the polarizability components $\alpha_{||}$ (R), and $\alpha_{\perp}$ (R) and if one knows the vibrational wavefunctions Ψ_{VJ} and $\Psi_{V+1,J}$ as well as the scattering frequency ν_{scatt}, one can determine the Raman scattering cross section for a given transition from one electronic-vibrational-rotational state to another. In the next section we present results of such calculations for selected diatomic molecules of interest in combustion analysis.

V. CALCULATED RAMAN-SCATTERING CROSS-SECTION RESULTS

The determination of the Raman scattering cross section for a particular molecule proceeds in several steps: 1) solve for the wavefunction $\Psi_e(\vec{r},R)$ in the absence and presence of an electric field; 2) use the wavefunctions from step (1) to find the polarizability as a function of internuclear separation; 3) use the electronic energy found in step (1) to find the vibrational wavefunctions $\Psi_{VJ}(R)$; 4) use the polarizability and the vibrational wavefunctions to find the transition probability $|M_0|^2$, and 5) substitute the value of $|M_0|^2$ into Eq. (4) to obtain the intensity of the light scattered by the molecules.

The determination of the electronic wavefunction $\Psi_e(\vec{r},R)$ involves the application of extremely sophisticated electronic structure codes, the utilization of which has only become possible with the advent of high-speed computers. These methods and the resulting electronic wavefunctions will be presented in another publication. In this report we present the polarizabilities obtained from these electronic wavefunctions and the resulting Raman scattering cross sections. As examples, we consider the diatomic molecules H_2, LiH, OH, N_2, NO, O_2 and O_2^*. (O_2^* denotes the first electronically excited state of O_2.)

First, we present the results for the total electronic energy U(R) as a function of internuclear separation. Since we are concerned with molecular vibration of small amplitude, we need calculate U(R) only for $R \approx R_e$. For this reason, we calculate U(R) at five internuclear distances spaced about the equilibrium bond distance R_e. To simplify the interpretation, we have fitted the calculated points to a Morse potential,

$$U(R) = D_e \{1 - \exp[-a(R - R_e)]\}^2 + U_e \tag{13}$$

The choice of this analytic form is somewhat arbitrary, although it does have the general shape expected for a diatomic molecule.[5] In Figure 4 we display the results of our calculations.

From the parameters a and D_e of the Morse potential, we are able to determine the harmonic frequency ω_e and the anharmonicity $\omega_e x_e$ of the potential energy curves. The harmonic frequency is given by

$$\omega_e = \sqrt{\frac{2D_e}{M_R}}\ a, \tag{14}$$

where M_R is the reduced mass of the molecule. The anharmonicity is given by

$$\omega_e x_e = \frac{\omega_e^2}{4D_e} \tag{15}$$

The vibrational frequency ν_{mol}, corresponding to a transition between vibrational states $\Psi_{V,J}$ and $\Psi_{V+1,J}$, is given by

$$\nu_{mol} = \omega_e - 2\omega_e x_e (V + 1). \tag{16}$$

---

5. G. Herzberg, Spectra of Diatomic Molecules, D. Van Nostrand, Inc. New York, (1950).

In Table I we compare our results with experiment for the equilibrium separation R_e, the frequency ω_e, and the anharmonicity $\omega_e x_e$. We have treated the molecules in Table I, including important correlation effects which can also be applied to larger molecular systems of interest in flame analysis; e.g., HO_2, H_2CO, and NH_2. The agreement displayed in Table I suggests the validity of this approach.

Having calculated the electronic wavefunction we can obtain the electronic polarizability as a function of internuclear separation. If we denote the ground electronic state in the absence of an applied field by $\Psi_e^{(o)}(\vec{r},R)$ and in the presence of the field without the superscript we can write the electronic polarizability for unit magnitude external field as

$$\alpha = \int \Psi_e(\vec{r},R) \sum_{i=1}^{N_e} ez_i \, \Psi_e(\vec{r},R) \, d\vec{r} - \int \Psi_e^{(o)}(\vec{r},R) \sum_{i=1}^{N_e} ez_i \, \Psi_e^{(o)}(\vec{r},R) \, d\vec{r} \qquad (17)$$

Table I

Comparison of Theoretical and Experimental Molecular Parameters For Various Diatomic Molecules. Experimental Values taken from Ref. 5.

	EQUILIBRIUM SEPARATION		HARMONIC FREQUENCY		ANHARMONICITY	
	R_e (Å)		ω_e (CM^{-1})		$\omega_e x_e$ (CM^{-1})	
	Theor.	Exp.	Theor.	Exp.	Theor.	Exp.
H_2	0.76	0.74	4223	4395	163	118
LiH	1.65	1.60	1293	1406	30	23
OH	0.99	0.97	3631	3735	110	83
N_2	1.12	1.09	2374	2360	12	14
NO	1.17	1.15	1983	1904	13	14
O_2	1.23	1.21	1622	1580	12	12
O_2^*	1.24	1.22	1568	1509	12	12

where $\sum_{i=1}^{N_e} e_i z_i$ represents the electronic dipole moment operator. For homonuclear diatomic molecules, the second term in Eq. (17) vanishes by symmetry.

An alternative approach (and the one actually used by us) in determining the polarizability is the use of the relationship

$$U(R)|_{Field} = U(R)|_{\substack{No \\ Field}} - \vec{\mu}\cdot\vec{E} - \frac{1}{2}\vec{E}\cdot\overleftrightarrow{\alpha}\cdot\vec{E} + \ldots \tag{18}$$

for the change in the electronic energy in the presence of an applied electric field $\vec{E}$. In Eq. (18) $\vec{\mu}$ is the permanent dipole moment of the molecule (nonzero only if the molecule has no center of symmetry).

The use of Eq. (18) to determine the polarizability is valid only for small fields $\vec{E}$ since Eq. (18) represents a power series expansion in the electric field. [The expression $\overleftrightarrow{\alpha}\cdot\vec{E}$ in Eq. (18) corresponds to the induced dipole moment. This expression also is valid only for small fields.] For such small fields, the energy change is quite small. For example, for O_2, the energy change upon application of a suitably small field is one-millionth that of the total energy of the molecule. Thus, the energy change (and hence the polarizability) is an extremely demanding test of the theoretical approach and makes the polarizability calculation very difficult.

Using Eq. (18) we have calculated $\alpha(R)$ for five spacings about the equilibrium internuclear separation. We have fit our results (using a least-squares fitting technique) to the quadradic form

$$\alpha(R) = A_0 + A_1 (R - R_e) + \frac{A_2}{2}(R - R_e)^2. \tag{19}$$

The resulting curves and calculated points are shown in Figure 5 while the parameters A_0, A_1 and A_2 are displayed in Table II. The main point to notice from

the Table is the dominant contribution of the parallel component to the total polarizability derivative (A_1). Since it is the square of this quantity (see Eq. 11) which determines the scattering cross section, one sees that it is primarily the change of the parallel component of polarizability which determines the Raman scattering intensities. Notice that for N_2, NO, O_2, and O_2^* the parallel derivative is an order of magnitude larger than the perpendicular derivative.

The next step in the program involves determining the wavefunction $\Psi_{VJ}(R)$. This wavefunction is a solution to the differential equation

$$-\frac{1}{2M_R}\frac{d^2\Psi_{VJ}(R)}{dR^2} + \left\{ U(R) + \frac{J(J+1)}{2M_R R^2} \right\} \Psi_{VJ}(R) = E_{VJ}\Psi_{VJ}(R) \tag{20}$$

Table II

Polarizability Parameters for Various Diatomic Molecules

Molecule	A_0		A_1		A_2	
	Parallel	Perpendicular	Parallel	Perpendicular	Parallel	Perpendicular
H_2	6.17	4.13	6.04	2.58	3.7	0.2
LiH	33.73	38.85	25.11	11.40	21.2	9.1
OH	6.95	3.92[a]	6.31	0.18[a]	5.7	0.6[a]
N_2	13.23	6.89	9.93	1.13	-1.1	-2.9
NO	12.69	5.82[a]	9.53	0.70[a]	0.5	-1.3[a]
O_2	12.84	4.18	9.18	0.20	-0.9	-0.5
O_2^*	11.22	4.09	7.34	0.20	0.1	-0.1

[a]The ground states of OH and NO are $^2\Pi$ states. The perpendicular parameters tabulated represent averages of the two perpendicular components.

where M_R is the reduced mass of the molecule, U(R) is the electronic energy as a function of internuclear separation, J is the quantum number specifying the rotational state of the molecule, and E_{VJ} is the sum of vibrational and rotational energy for the state (V,J). Notice that the energy $U(R) + J(J+1)/2M_R R^2$ acts as an effective potential energy governing the motion of the nuclei. For the molecules considered here, U(R) is the dominant contribution to this effective potential energy.

We have solved this differential equation using a modified version of a computer code written by J. F. Lathrop.[6] As illustrated in Figure 6, we show the wavefunctions $\Psi_{VJ}(R)$ for the H_2 molecule for J=0 and V=0,1,2. Superimposed on the plot is the effective potential U(R). Each wavefunction is plotted on an axis corresponding to the vibrational energy of that vibrational state.

Finally, we can proceed to determine the scattering cross sections, Eq. (11), using the results of Eq. (18) and Eq. (20) substituted into Eq. (13). Since the cross section depends upon the incident photon frequency, we have used the Ar ion laser frequency appropriate for Sandia's combustion flame analysis. One could use the wavefunctions obtained above to calculate transition probabilities between specific states $(V,J) \rightarrow (V',J')$. In our calculation of the scattering intensity, we have treated the potential $\{U(R) + \frac{J(J+1)}{2M_R R^2}\}$ as strictly parabolic. [That this is a good approximation can be seen by comparing the harmonic frequency ω_e and the anharmonicity $\omega_e x_e$ in Table I.] In this case, only the A_1 of Table II [corresponding to α_1 of Eq. (7)] contributes to the Raman scattering cross section. Since Sandia's experimental arrangement

6. J. F. Lathrop, private communication.

measures scattered light only at right angles to the incident light, it is the differential Raman scattering cross section which is needed. Thus, Eq. (11) is replaced by

$$\frac{\partial\sigma_{Raman}}{\partial\Omega} = \frac{4\pi^3}{c^4}(V+1)\frac{\nu^4_{scatt}}{M_R\,\nu_{mol}}\left[\frac{1}{9}\left(A_{1_{||}} + 2A_{1_{\perp}}\right)^2 + \frac{7}{45}\left(A_{1_{||}} - A_{1_{\perp}}\right)^2\right] \quad (21)$$

The resulting differential Raman scattering cross sections for the ground vibrational states (V = 0) of H_2 and N_2 molecules are presented in Table III. The essentially exact results for H_2 and experimental determination for N_2 are presented for comparison. With regard to combustion flame analysis, only the relative differential Raman scattering cross sections are necessary. Therefore, we have tabulated the relative cross sections for LiH, OH, N_2, NO, O_2, and O_2^* (with respect to the H_2 molecule) in Table IV. Available experimental data are also presented in Table IV for comparison. Notice the very good agreement for all except the NO molecule. Part of the discrepancy may be due to the difficulty of measuring <u>isolated</u> NO molecules, since these molecules tend to form $(NO)_2$ dimers.

Table III

Absolute Differential Raman Scattering Cross Sections[a]

Molecule	Present Theory 10^{-31} cm^2/ster-mol	Literature 10^{-31} cm^2/ster-mol	
H_2	11.2	14.7	Exact[b]
N_2	3.9	3.3 ± 1.1	Exp[d]
	5.2 [c]	4.3	Exp
		5.5 ± .3	Exp
		5.6 ± 2.2	Exp
		5.5	Exp
		4.8	Exp

[a] Cross sections correspond to the ground state (V = 0) to the first excited state (V = 1) vibrational transition.

[b] W. Kolos and L. Wolniewicz, J. Chem. Phys. 46, 1426 (1967).

[c] Using the exact cross section for H_2 and the theoretical ratio of N_2 to H_2 (see Table IV).

[d] Experimental results quoted by W. R. Fenner, H. A. Hyatt, J. M. Kellam and S. P. S. Porto, J. Opt. Soc. 63, 77 (1973).

Table IV

Differential Raman Cross Sections (Relative to H_2) for Several Diatomic Molecules

	Calculated	Experimental Results[a]			
H_2	1.0	1.0	1.0	1.0	1.0
LiH	58.	Not measured			
OH	.48	Not measured			
N_2	.35	.36	.37	.43	.42
NO	.40	...	...	.24	.11
O_2	.43	.43	.44	.52	.54
O_2*	.29	Not measured			

[a]Experimental results quoted by W. R. Fenner, H. A. Hyatt, J. M. Kellam and S. P. S. Porto, J. Opt. Soc. 63, 77 (1973).

Discussion

The theoretical calculation of Raman scattering cross sections is an extremely difficult problem. It requires the calculation of the derivative of the polarizability of a molecule when the calculation of the polarizability itself is an extremely difficult problem. In fact, we have found that the Hartree-Fock wave function, used as a starting point for perturbation theory, is not sufficiently accurate or reliable for polarizability derivatives. Furthermore, the cross section is proportional to the square of the polarizability derivative which further increases the relative error. Therefore, we have had to use quantum mechanical methods which go beyond Hartree-Fock. The results presented in the previous section (Table III and IV) represent an approach which goes beyond Hartree-Fock by including those additional configurations which describe molecular dissociation (it is these configurations which are most sensitive to changes in the internuclear separation). Furthermore, the coupled equations are solved exactly rather than by perturbation theory and are solved self-consistently. We feel that this approach provides reliable cross sections (as exemplified by Table IV) and can be applied to larger polyatomic systems while remaining within the limitations of present day computers (on the level of the CDC7600). This approach tends to underestimate the absolute cross section (the cross section for H_2 (Table III) is too small by 24%). However, we see that the absolute cross sections obtained theoretically are well within the accuracy obtained experimentally. Furthermore, this error is minimized when relative cross sections are considered (see Table IV).

In Table IV we see that the theoretical relative cross sections vary by over two orders of magnitude. The theory is in very good agreement with experiment for H_2, N_2 and O_2. On the other hand, the results for NO are in

agreement only to within a factor of two or four (even the experimental results do not agree). We are not able to determine at this time whether the theoretical or the experimental cross section for NO is more reliable.

One also sees from Table IV that there are no experimentally determined cross sections for LiH, OH, or O_2^*. The reason is that these molecular species are very unstable and reactive making it difficult to isolate these species in large enough concentrations to make an experimental determination of the cross section. However, a molecular radical such as OH plays an important role as an intermediate in combustion flames. Thus, it is essential to determine its cross section. Theoretically, an unstable molecule such as OH is no more difficult to treat than a stable molecule such as N_2. This illustrates the great usefulness of the theoretical approach. Theory can provide absolute cross sections for important reaction intermediates occurring in combustion flames. As a second example, we have calculated the cross section for the electronically excited state of O_2. This excited state of O_2 should play an important role as an intermediate in combustion flames. Its cross section, however, can only be determined theoretically since it is very short-lived.

Besides being able to calculate theoretical cross sections, our investigation of polarizability derivatives has provided insight into making qualitative predictions of cross sections of new molecular species. The frequency ν_{mol} is distinctive of a localized bond (such as the O-H stretching mode in OH, H_2O and HO_2). One might expect the polarizability to follow a similar pattern. Based on the similarity of the localized electronic structure, one would expect the cross section for the O-H stretching mode to be quite similar for OH, H_2O, HO_2 or CH_3OH. Furthermore, the close similarity in the electronic structure between O_2 and N_2 would lead one to expect similar

cross sections. Thus, one would expect the cross section for the N-H stretching mode in NH or NH_2 to be fairly similar to OH. These are qualitative predictions which should be accurate to within a factor of two.

So far we have considered Q-branch transition between the ground and first excited vibrational state ($V = 0 \rightarrow V = 1$). For temperature profile measurements, one also monitors transitions which originate from excited vibrational states; e.g., ($V = 1 \rightarrow V = 2$). This requires knowledge of the frequency shift ν_{mol} and the differential cross section appropriate to such transitions. From Table I we see that our theoretical approach provides accurate values for these frequency shifts as given by Eq. (16). The facts that the polarizability components are essentially linear functions of internuclear separation and that the anharmonicity is small justifies the use of Eq. (21) for vibrationally-excited state transitions.

In conclusion, we have demonstrated the capability to calculate Raman scattering cross sections which can be used with confidence in combustion flame analysis. Our approach is readily applicable to larger polyatomic molecules of interest in combustion flame analysis while maintaining a comparable level of accuracy.

Figure Captions

Fig. 1 The scattering geometry for light scattering experiments employing observation at right angles to the incident beam.

Fig. 2 Schematic illustration of polarization of incident and scattered radiation.

Fig. 3 Stokes Raman Scattering. ν_{inc} is the frequency of the incident laser light, ν_{scatt} is the frequency of the scattered light, and ν_{mol} is the frequency shift corresponding to the change in the internal energy state of the molecule going from the ground vibrational state (V = 0) to the first excited vibrational state (V = 1).

Fig. 4 The total electronic energy U(R) for several diatomic molecules. The solid curves are Morse potential curves fitted to the calculated points denoted by asterisks.

Fig. 5 The electronic polarizability $\alpha(R)$ for several diatomic molecules. The solid curves denote the parallel component $\alpha_{||}(R)$; the dashed curve denotes the perpendicular component $\alpha_{\perp}(R)$.

Fig. 6 Vibrational wave functions for H_2 molecule. The dashed curve is the electronic energy U(R). The wave functions are plotted so that the function asympotically approaches the corresponding vibrational energy.

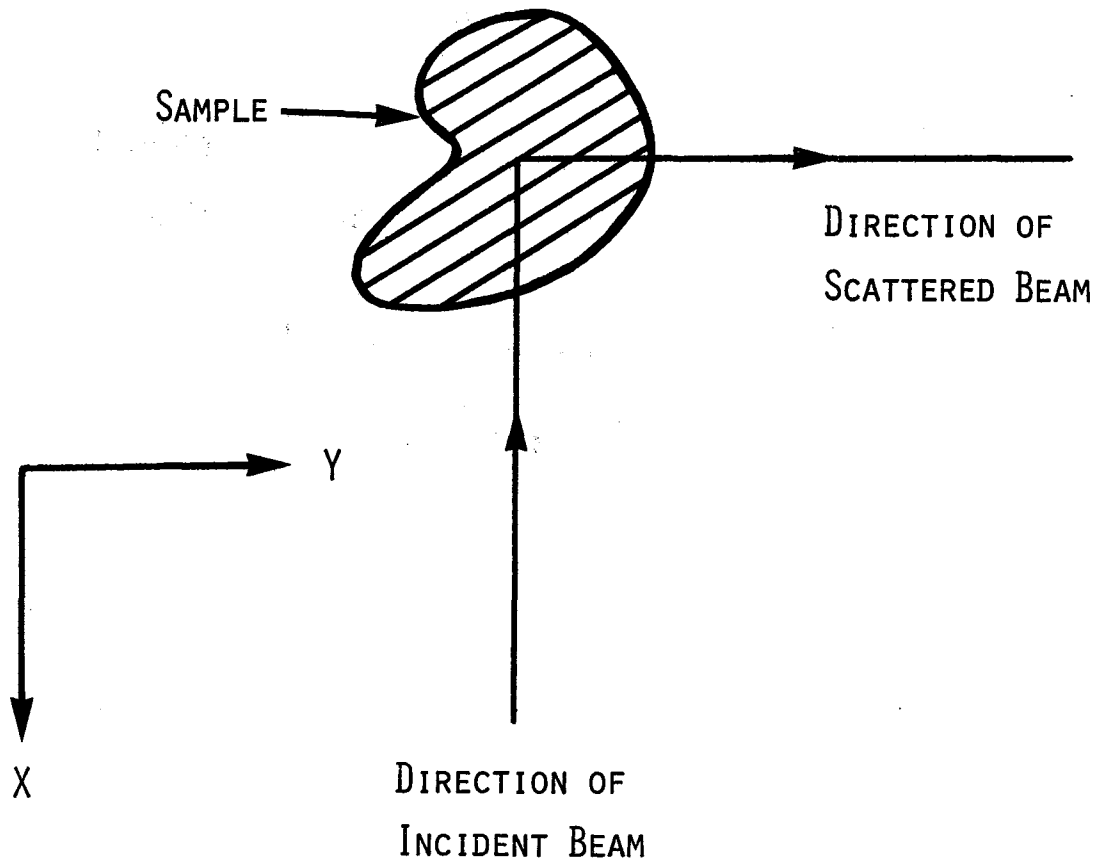
SAMPLE
DIRECTION OF
SCATTERED BEAM
Y
X
DIRECTION OF
INCIDENT BEAM

FIGURE 1

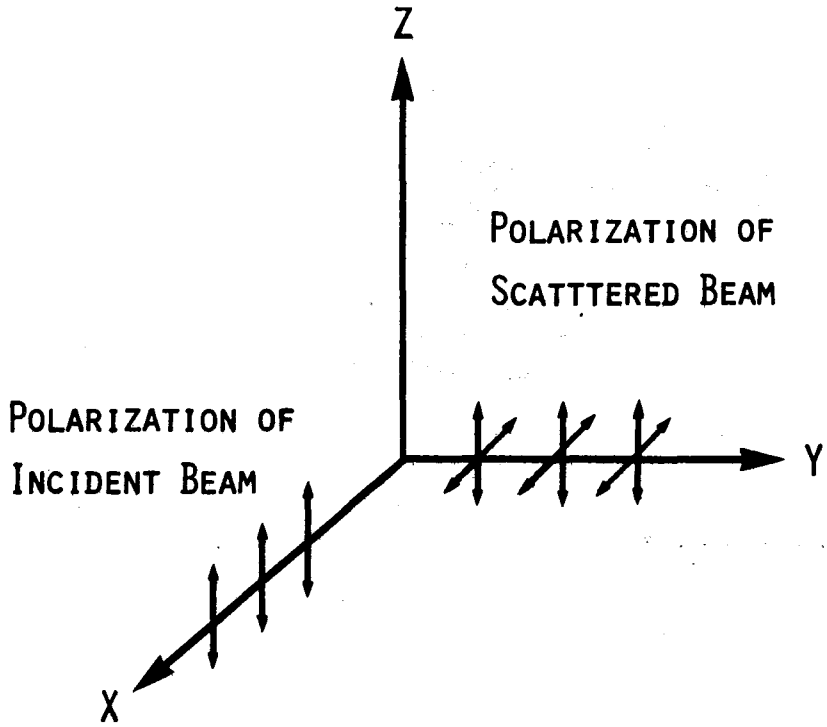
Z
Polarization of
Scatttered Beam
Polarization of
Incident Beam
Y
X

Figure 2

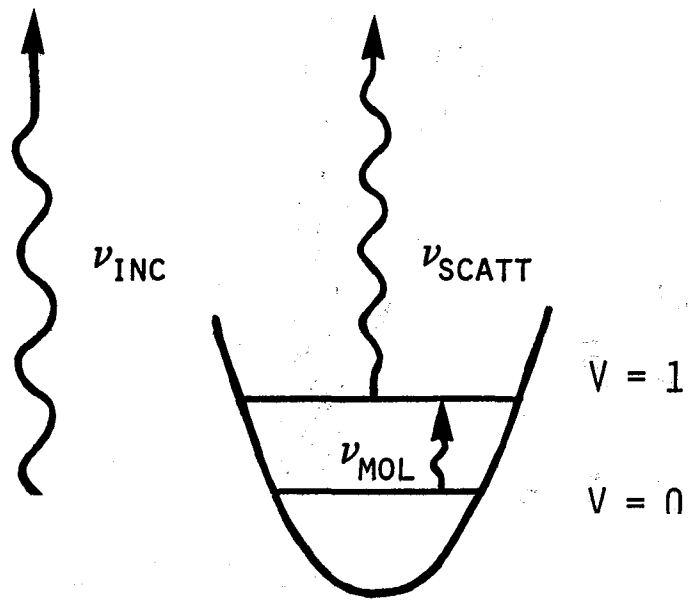

FIGURE 3

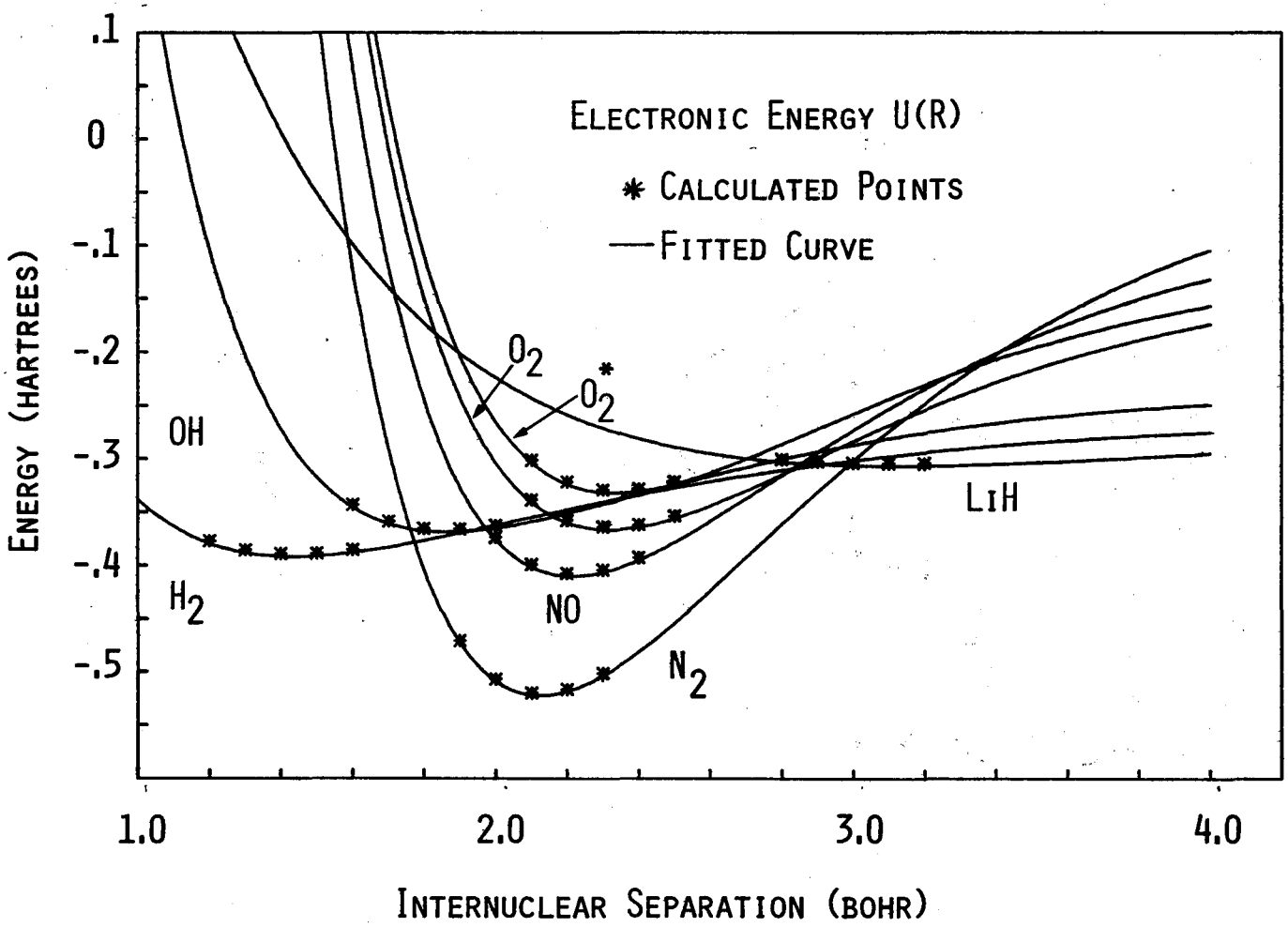
ELECTRONIC ENERGY U(R)
* CALCULATED POINTS
— FITTED CURVE
ENERGY (HARTREES)
.1
0
-.1
-.2
-.3
-.4
-.5
1.0
2.0
3.0
4.0
INTERNUCLEAR SEPARATION (BOHR)
OH
H_2
O_2
O_2^*
NO
N_2
LIH

FIGURE 4

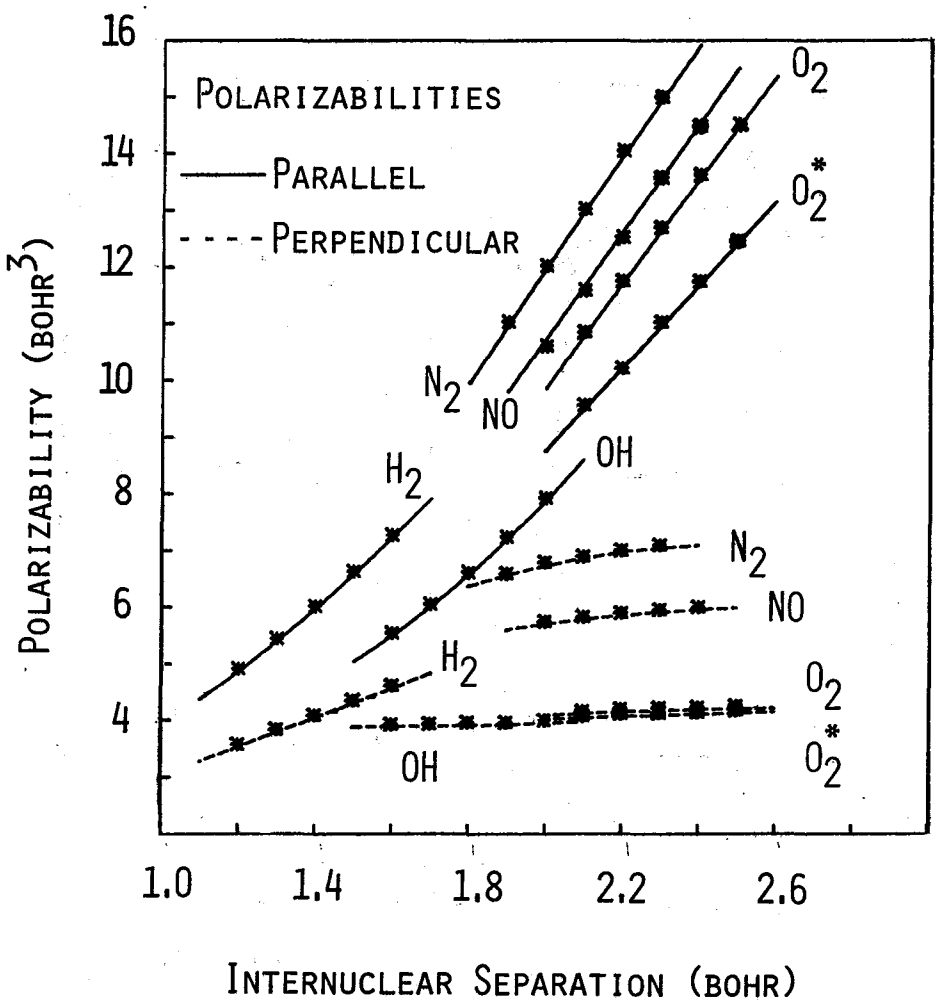
POLARIZABILITIES
PARALLEL
PERPENDICULAR
POLARIZABILITY (BOHR^3)
16
14
12
10
8
6
4
1.0
1.4
1.8
2.2
2.6
INTERNUCLEAR SEPARATION (BOHR)
N_2
NO
O_2
O_2^*
H_2
OH
N_2
NO
H_2
O_2
OH
O_2^*

FIGURE 5

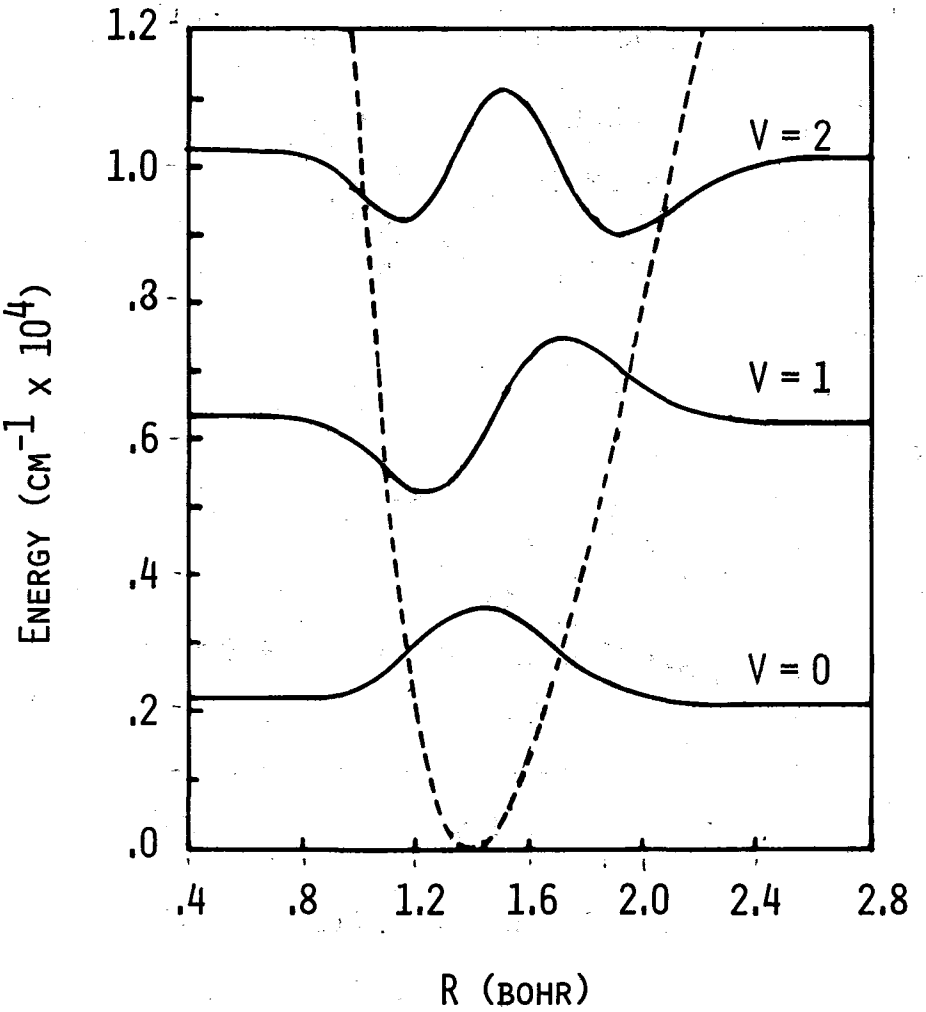

FIGURE 6

UNLIMITED RELEASE

INITIAL DISTRIBUTION

General Electric Corporate
Research and Development
P. O. Box 8
Schenectady, New York 12301
Attn: M. Lapp

Queens College
Physics Department
Flushing, New York 11367
Attn: C. R. Fischer

U. S. Energy Research and Development Administration
Washington, D.C. 20545
Attn: J. A. Belding
J. Hudis
J. S. Kane
J. V. Martinez
E. S. Pierce
D. K. Stevens
M. C. Wittels

University of California
Department of Mechanical Engineering
Berkeley, California 94720
Attn: J. Dailey

United Technologies Research Center
East Hartford, Connecticut 06108
Attn: A. Eckbreath

A. Narath, 5000
J. K. Galt, 5100
J. E. Schirber, 5150
A. C. Switendick, 5151
E. H. Beckner, 5200
J. B. Gerardo, 5210
E. J. McGuire, 5211
K. J. Touryan, 5260
T. A. Green, 5261
J. M. Peek, 5261

T. B. Cook, Jr., 8000; Attn: L. Gutierrez, 8100
C. H. DeSelm, 8200
W. C. Scrivner, 8400

A. N. Blackwell, 8110
D. Hartley, 8115 (19)

INITIAL DISTRIBUTION (Cont'd.)

B. F. Murphey, 8300; Attn: R. H. Meinken, 8310
T. S. Gold, 8320
G. W. Anderson, 8330
J. F. Barham, 8360

W. Bauer, 8334
J. Vitko, 8334
P. L. Mattern, 8334

J. L. Wirth, 8340; Attn: A. R. Willis, 8344
F. J. Murar, 8345
O. H. Schreiber, 8346

W. D. Wilson, 8341
C. F. Coll, 8341 (15)
C. F. Melius, 8341 (15)
E. H. Barsis, 8342
C. M. Hartwig, 8342
L. A. Rahn, 8342
R. W. Schmieder, 8342

Technical Publications and Art Division, 8265, for TIC (2)
F. J. Cups, 8265/Library Systems & Technical Processes Division, 3141
Library Systems & Technical Processes Division, 3141 (4)
Library and Security Classification Division, 8266-2 (5)